JOURNAL OF SPACECRAFT AND ROCKETS
Vol. 29, No. 3, May-June 1992

Local Bridging to Predict Aerodynamic Coefficients in Hypersonic, Rarefied Flow

J. Leith Potter* and Steven W. Peterson†
Vanderbilt University, Nashville, Tennessee 37235

A computational method is given for the prediction of local pressure and viscous shear stress on windward surfaces of convex, axisymmetric or quasi-axisymmetric, hypersonic bodies in the transitional, rarefied flow regime. Overall aerodynamic forces and moments are computed by integration of the local quantities. The method is based on a correlation of local pressure and shear stress computed by the direct simulation Monte Carlo (DSMC) numerical technique for cold-wall, real-gas conditions and some supplemental data from low-density, hypersonic wind tunnels. Two-dimensional shapes and leeward surfaces are not included in the scope of the method as it is presented here. Results are compared with DSMC and viscous shock layer computations for both local and overall coefficients. Also included are sphere and blunt cone drag obtained from both computation and experiment, as well as lift and pitching moment coefficients for the NASA Aeroassist Flight Experiment vehicle at various angles of attack. It appears that the method presented here will prove adequate for relatively bluff bodies approximately defined by wetted length-to-nose radius ratios of less than 10.

Nomenclature

A = reference area
C_D = drag coefficient, drag/$[(\rho_\infty U_\infty^2/2)A]$
C_f = friction coefficient, $\tau/(\rho_\infty U_\infty^2/2)$
C_L = lift coefficient, lift/$[(\rho_\infty U_\infty^2/2)A]$
C_M = pitching moment coefficient, moment/$[(\rho_\infty U_\infty^2/2)Al]$
C_p = pressure coefficient, $(p-p_\infty)/(\rho_\infty U_\infty^2/2)$
E = fraction of molecules specularly reflected
H = enthalpy
Kn = Knudsen number, λ/characteristic length
l = reference length
M = Mach number
p = pressure
R = radius of curvature
Re = Reynolds number
S = molecular speed ratio, $M_\infty\sqrt{\gamma/2}$
T = temperature
U = velocity
V = $M_\infty/\sqrt{Re_\infty}$
w = wetted length from stagnation point to local body station
y = see Eq. (5)
Z = simulation parameter
α = angle of attack
γ = ratio of specific heats
θ = angle between local surface normal and freestream velocity vector
λ = mean free path
μ = coefficient of absolute viscosity
ρ = fluid density
τ = fluid shear stress
ω = exponent in viscosity-temperature relation, $\mu \sim T^\omega$

Subscripts

b = base
e = outer edge of boundary layer
fm = free-molecular flow
i = inviscid flow
n = nose
o = total
s = shock process
w = wall condition
2 = downstream side of normal shock
∞ = freestream condition

Introduction

IT is well known that neither the continuum-flow equations nor the collisionless-flow equations are valid throughout the transitional flow regime encountered by vehicles operating at high altitudes in planetary atmospheres. At this time it appears that the direct simulation Monte Carlo (DSMC) method is the most accurate and general procedure for computing local and overall aerodynamic coefficients on typical aerospace vehicles in hypersonic, rarefied, or transitional flow. However, for good results, particularly at higher densities, that technique requires a great amount of computer time and a skillful practitioner. A reasonably accurate, simpler calculation is very useful if large numbers of aerodynamic force and moment predictions under varying speed and density conditions are needed. In the past, several bridging equations have been used for predicting overall drag coefficients of bluff, convex shapes, and more recently this approach has been extended in efforts to predict local as well as overall aerodynamic coefficients. Bridging, in this context, describes the procedure that involves the following steps: 1) plotting an experimentally determined overall coefficient, say C_D, as a function of an appropriate simulation parameter such as Re_2, with the limits on the coefficient at Re_2 of infinity and zero computed by inviscid and free-molecular theory, respectively; 2) fitting an equation to the correlated data, making it match the computed, extreme points; and 3) then using this bridging equation to predict the particular coefficient at other values of the simulation parameter.

Greater flexibility is gained by using a normalized aerodynamic coefficient, e.g., $\overline{C_D} = (C_D - C_{Di})/(C_{Dfm} - C_{Di})$.[1] When that has been done, it has often been assumed that the bridg-

Presented as Paper 91-0336 at the AIAA 29th Aerospace Sciences Meeting, Reno, NV, Jan. 7-10, 1991; received Aug. 9, 1991; revision received Dec. 16, 1991; accepted for publication Jan. 3, 1992.

*Research Professor, Department of Mechanical Engineering. Fellow AIAA.
*Assistant Professor, Department of Mechanical Engineering.

ing equation is valid even if body shape and surface conditions differ from the cases that provided the correlated data. For obvious reasons, mixed results have been obtained.

An improvement in generality and accuracy may be gained by recourse to a localized bridging approach.[2,3] That is, bridging between inviscid and free-molecular values is utilized to get local pressures and shear stresses on elements of body surface. Overall coefficients are then obtained by integration. The earlier methods have been based on a mixture of older computed and experimental data of limited scope (e.g., flat-plate data) to provide the bridging formula.

The present paper describes a local bridging (LB) method wherein local pressure and shear are based on correlation of those quantities as calculated for spherical shapes by the DSMC method[4] in the transitional rarefied flow regime. A condition associated with the use of solutions for spheres is the positive velocity gradient throughout the windward-side local flow. That is one reason that the bluff-body specialization of the present, approximate method is emphasized. This type of body and flowfield is characteristic of "aerobrake" or "aeroassist" re-entry vehicles epitomized by the Aeroassist Flight Experiment (AFE) and Aeroassisted Orbital Transfer Vehicle (AOTV) designs currently being studied by NASA. Those programs provided the primary motivation for this work. However, it is shown that extension of this method to blunt or sharp conical bodies seems promising. An outline of the method and examples of results follow. Although local pressure and shear are predicted, it is emphasized that the principal goal is the improvement of predictions of overall aerodynamic coefficients.

Analysis

The principal part of this problem is represented by the large variation in skin friction coefficient as the transitional flow regime is traversed. Computed pressure, for equal conditions, is not as greatly different when either inviscid or diffusely reflected, free-molecular flow is assumed. Therefore, most of this discussion concerns the viscous shear stress, and a pressure bridging equation will be given after the viscous shear parameter is defined.

Transitional Skin Friction

It was decided to combine a continuum, laminar, compressible-flow boundary-layer analysis and free-molecular flow theory to establish the form of the basic correlation parameter and to use the free-molecular flow theory to get the baseline value of the local shear stress that would be modified to yield the local shear in transitional flow. Thus, we start with the relationships[5]

$$C_{fw} = 2\tau/(\rho_w U_e^2)$$

$$= \text{combination of correlation parameters}/\sqrt{Re_w} \quad (1)$$

and

$$Re_w = (\rho_w U_e w/\mu_w)$$

After converting to the more conventional skin friction coefficient,

$$C_f = C_{fw}(\rho_w/\rho_\infty)(U_e/U_\infty)^2$$

making the substitutions

$$\rho_w = \rho_\infty(p_w/p_\infty)(T_\infty/T_w)$$

$$\mu_w = \mu_\infty(T_w/T_\infty)^\omega$$

and using the Newtonian flow approximation,

$$p_w/p_\infty = [(\gamma_s + 3)/(\gamma_s + 1)](\gamma_\infty/2)M_\infty^2 \cos^2\theta$$

$$\equiv p_e/p_\infty$$

it is found that

$$C_f(Re_\infty)^{1/2} \sim (f)\{M_\infty \cos\theta(T_\infty/T_w)^{(1-\omega)/2}$$

$$\times [(\gamma_\infty/2)(\gamma_s + 3)/(\gamma_s + 1)]^{1/2}(U_e/U_\infty)^{3/2}\} \quad (2)$$

The symbol $\sim$ means "varies as," and f represents the undefined correlation parameters in Eq. (1).

There is a real-gas factor represented by the term involving γ_s. This has been distinguished from γ_∞ because γ_s is an "effective" value connected with the pressure rise at the stagnation point, whereas γ_∞ is a freestream property. Fortunately, the range of values of the γ_s term, $\sqrt{(\gamma_s + 3)/(\gamma_s + 1)}$, for $1 \le \gamma_s \le 1.4$, is modest. Because of that, it is treated as a constant and omitted hereafter.

The velocity ratio in Eq. (2) may be expressed as

$$U_e/U_\infty = [(H_o - H_e)/(H_o - H_\infty)]^{1/2}$$

$$\approx (1 - H_e/H_o)^{1/2}$$

It will be noted that enthalpy is an extensive fluid property and this relation is valid if equilibrium exists at stations e and o. Hereafter, the velocity ratio is regarded as a function of θ only.

When $S_\infty^2 \cos^2\theta \gg 1$, free-molecular flow theory gives

$$C_{ffm} \approx 2(1 - E)\sin\theta\cos\theta \quad (3)$$

Then, from Eqs. (2) and (3), omitting the functions of specific heat ratio that may be restored if other than the Earth's atmosphere is of concern,

$$C_f/C_{ffm} \sim \frac{(f)\{[M_\infty/\sqrt{Re_\infty}](T_\infty/T_w)^{1-\omega)/2}(U_e/U_\infty)^{3/2}\}}{[(1 - E)\sin\theta]} \quad (4)$$

The fraction of molecules reflected specularly from the solid surface, E, would be 1.0 if the assumption of fully specular reflection is made. Experience, such as it is, suggests that $E = 1$ is unrealistic, and diffuse reflection or $E = 0$ is the most often assumed model of gas/surface interaction when normal and tangential momentum transfer are estimated. It is conceded that $0 < E(\theta) < 1$ probably is the correct description, but sufficient data for actual flight conditions are lacking. Hurlbut has discussed this subject in greater detail.[6]

It remains to evaluate f in Eq. (4). It combines the several pressure gradient and heating rate parameters utilized to correlate similar solutions of thin, continuum, compressible, laminar boundary layers.[5] For the blunt, convex, cold-wall, hypersonic bodies of concern in the present discussion, in the context of the Newtonian flow model, the pressure and velocity distributions are considered to be simple functions of θ. Thus, the quantity $(U_e/U_\infty)^{3/2}/\sin\theta$, which is seen in Eq. (4), readily may be expressed as a function of θ by using a Newtonian flow approximation. However, local pressure gradient is one of the factors in C_f, so an $f(\theta)$ that yields a successful correlation must represent the combined roles of local velocity and velocity gradient. It was found by examination of the DSMC results for the spheres that a good correlation may be achieved by adopting $f(\theta) = 1 + \sin\theta$ for $\theta < 84$ deg, where $f(\theta)$ combines all of the variables dependent on θ. Very high angles (low incidence) constitute a special case addressed later. Considering that the $(1 + \sin\theta)$ term is based on calculations for flow over spheres, and the form of Eq. (4) does not fully reflect certain transitional-flow characteristics, it must be anticipated that modifications should be necessary as we extend the application of this method to nonspherical shapes. These are also discussed later.

Full-scale flight and high-enthalpy wind-tunnel data correspond to the condition $H_w \ll H_o$. The DSMC calculations available for correlation also reflect this focus on the cold-wall condition of most practical interest. However, many of the

available wind-tunnel data do not satisfy the cold-wall criterion. Theoretical and experimental studies of skin friction under viscous-interaction conditions as well as correlations of sphere and cone drag coefficients have shown that some function involving H_w, H_e, H_o, or some reference enthalpy is a necessary part of any simulation parameter for transitional flows. The simplest form for such a term is H_w/H_o. Therefore, a term $(80H_w/H_o)^y$ is inserted in Eq. (4), and examination of sphere drag measurements has been the means to determine y. The number 80 appears because that is the ratio H_o/H_w for all of the DSMC sphere data underlying the basic correlation. It was desirable to index the enthalpy or heat transfer parameter to that condition. After study of sphere drag data from hypersonic wind tunnels where $0.086 \leq H_w/H_o \leq 1$, it was decided to make y dependent on the viscous interaction parameter V and the following empirical relation was adopted:

$$y = V^{2.7}/(V^{3.1} + 180) \tag{5}$$

The form of y has been devised so that the value tends to zero at either very low or very high values of V. In this sense, it is simply a bridging relation. Other forms could be designed to satisfy the same requirement.

Earlier in this discussion, the problem of correlating DSMC results for C_f when $\theta > 84$ deg was mentioned. This appears to arise from a combination of a real, physical phenomenon and scatter in the DSMC numerical results in regions of the flowfield where θ is very low (<6 deg) or very high (>84 deg). Because the former is believed to be wholly a computational shortcoming, associated with cell size and number of simulated molecules, it is ignored here. However, it is predictable that local forces in near-free-molecular flow overshoot the free-molecular flow result when surfaces are nearly parallel with freestream direction.[7] This is taken into account later. First, a correlation using the parameter Z is based on DSMC results for $0 \leq \theta \leq 75$ deg. The upper limit is conservative, but the subsequent modification adequately extends the coverage. After adding the factors discussed, the correlation or scaling parameter for skin friction ratio is denoted by the symbol Z, i.e.,

$$C_f/C_{ffm} \sim Z$$

where, assuming that $E = 0$ in Eq. (4),

$$Z = [M_\infty/(Re)^{1/2}](T_\infty/T_w)^{(1-\omega)/2}\,(1 + \sin\theta)(80H_w/H_o)^y \tag{6}$$

The viscosity-temperature exponent ω should be varied with temperature range to be more accurate in a specific case. For air or nitrogen, from Sutherland's equation, $\omega \approx 0.9$–1 in the range of T_∞ to T_w in unheated, low-density, hypersonic wind tunnels. However, $\omega \approx 0.7$–0.8 for the range of T_∞ to T_w representative of flight in the Earth's atmosphere. The data in Ref. 8 indicate that $\omega \approx 0.78$ may be more appropriate if a very wide range of temperatures is involved. In view of the relatively small influence of the exponent in Eq. (6), a value of 0.78 has been assumed hereafter for flight or high-enthalpy wind-tunnel cases, and a value of 0.90 is used for the unheated wind-tunnel case.

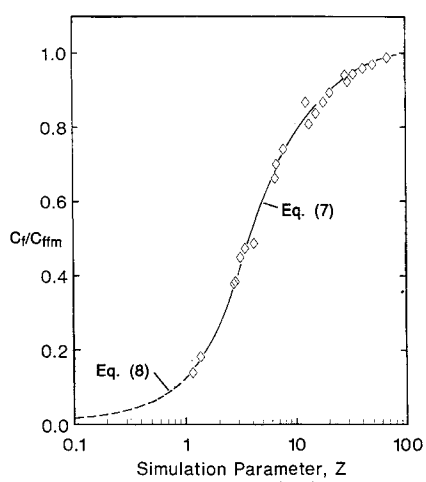

Fig. 1 Correlation of ratio of friction coefficients for $\theta < 75$ deg based on DSMC computations of Ref. 4.

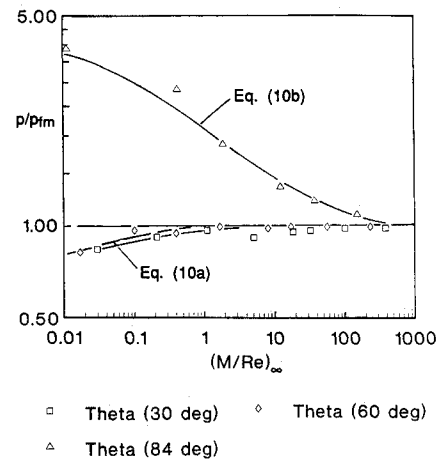

Fig. 2 Ratio of static pressures predicted by present method and DSMC computations of Ref. 4.

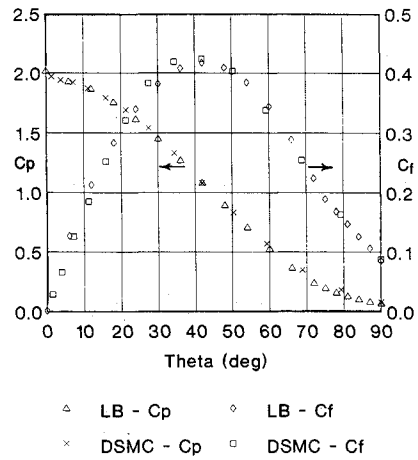

Fig. 3 Local shear and pressure coefficients on 1.6-m-diam sphere at 100-km altitude predicted by present method and DSMC computations of Ref. 4.

Figure 1 shows the correlation of the ratio C_f/C_{ffm} computed by the DSMC method[4] and plotted as a function of Z. Two equations have been fitted to the DSMC data to facilitate calculations of local and overall forces on bodies. For $Z > 1$ and $\theta \leq 75$ deg,

$$C_f/C_{ffm} = [0.24/(0.24 + Z^{-1.3})]^{1.25} \tag{7}$$

is a satisfactory analytic fit to the numerical results. For $0.1 < Z < 1$, based on the requirement to trend toward "thin-boundary-layer" results, at low Z, if $\theta \leq 75$ deg,

$$C_f/C_{ffm} = 0.1284Z \tag{8}$$

is the better equation. Below $Z \approx 0.1$, there is no need for the transitional-flow method, and one of the several continuum, thin-boundary-layer computation methods appropriate to the problem may be used. Two-dimensional bodies are not represented in Fig. 1. Although no study has been made, it is

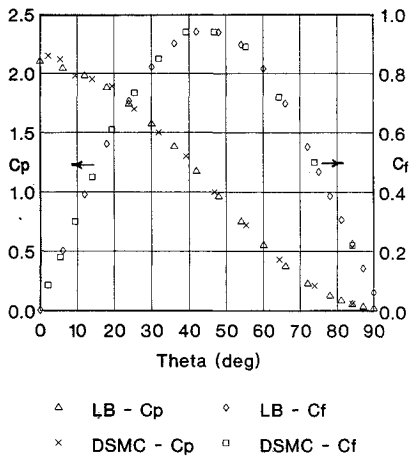

Fig. 4 Local shear and pressure coefficients on 1.6-m-diam sphere at 140-km altitude predicted by present method and DSMC computations of Ref. 4.

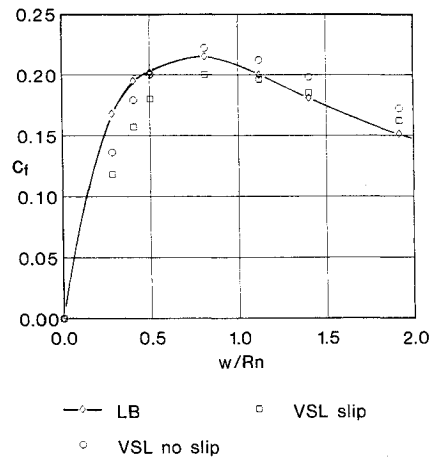

Fig. 5 Friction coefficients on hyperboloid predicted by present method and perfect gas viscous shock layer computations of Ref. 10.

expected that a similar but different curve would fit that case.

As remarked earlier, it was difficult to fit the very rapid increase of C_f/C_{ffm} as θ approached 90 deg in the overall correlation of DSMC data. It was found more satisfactory to limit the correlation to $\theta \leq 75$ deg, and to obtain C_f/C_{ffm} in the interval $75 < \theta \leq 90$ deg by linear interpolation between C_f/C_{ffm} for 75 deg, obtained from Eqs. (7-8), and the value for 90 deg obtained by modified equations. If $Z \geq 1$, the modified C_f/C_{ffm} for $\theta = 90$ deg is obtained by multiplying the right-hand side of Eq. (7) by the factor

$$[1 + 887.5/(7.46 + Z^{1.14})^2]$$

and, if $Z < 1$, the factor

$$[1 + 12Z^2]$$

is applied to Eq. (8). These multipliers have been chosen in order to fit the DSMC calculations for spheres when $\theta = 90$ deg.

The free-molecular skin friction coefficient is calculated by means of Eq. (9)[9];

$$C_{ffm} = \tau_{fm}/(p_\infty S_\infty^2)$$

$$\tau_{fm}/p_\infty = [(1 - E)S_\infty \sin\theta/\sqrt{\pi}]\{\exp(-S^2\cos^2\theta) + \sqrt{\pi}S_\infty \cos\theta[1 + \text{erf}(S_\infty \cos\theta)]\} \quad (9)$$

Transitional Pressure Ratio

The pressure coefficient at a point on a body varies between the continuum and free-molecule values throughout the transitional regime. Because the pressure is an "inviscid" quantity if the viscous interaction phenomenon is ignored, there is no reason to make it a function of the skin friction parameter Z when dealing with blunt-body flows. Freestream Knudsen number would seem a suitable parameter. It is proportional to M_∞/Re_∞ when the same length is the characteristic dimension in both Kn_∞ and Re_∞. Rather arbitrarily, we have chosen to correlate p/p_{fm} as a function of M_∞/Re_∞ for the purpose of estimating the variation of p/p_∞ in the transitional regime. Figure 2 shows a representative collection of DSMC results and the equation for pressure ratio used in our calculations.

When $p_i \leq p_{fm}$, the approximation used is

$$p/p_{fm} = 1 - (1 - p_i/p_{fm})/[1 + (0.6 + \theta)^4 (M_\infty/Re_\infty)^{1/2}] \quad (10a)$$

where θ is expressed in radians in both Eqs. (10) and (11). For large values of θ, local pressures and the corresponding values of p_i obtained from Eq. (11) may exceed p_{fm}. When $p_i > p_{fm}$, Eq. (10b) is used:

$$p/p_{fm} = 1 + (p_i/p_{fm} - 1)/[1 + 0.6(M_\infty/Re_\infty)^{1/2}] \quad (10b)$$

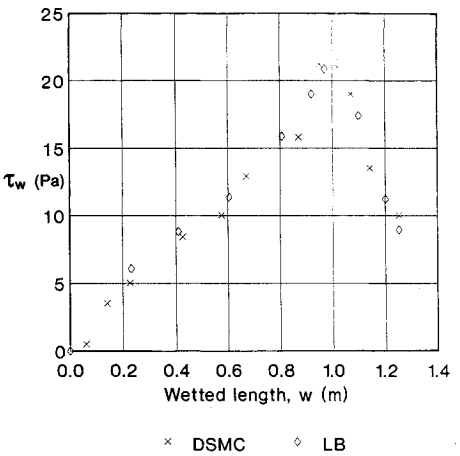

Fig. 6 Local shear stresses on surface of AFE spacecraft at 90-km altitude predicted by present method and DSMC computations of Ref. 11.

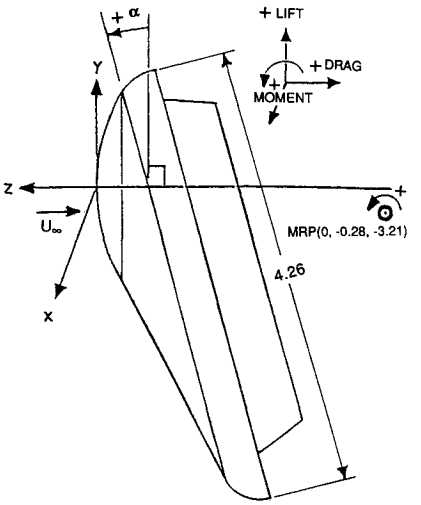

Fig. 7 NASA AFE vehicle profile, maximum diameter = 4.26 m.

The pressure corresponding to inviscid flow is approximated by

$$p_i/p_\infty = 1 + 1.895S_\infty^2(1 + 0.191\theta - 2.143\theta^2 + 1.564\theta^3 - 0.3340\theta^4) \quad (11)$$

Equation (11) is a curve fit based on a method of characteristics solution for hypersonic flow over a sphere. It will not be accurate in certain regions such as the area downstream of the junction of a spherical nose and conical afterbody. For calculations in those regions, it is better to use a computer code for inviscid flow over blunt bodies. For sharp-nosed cones, one may take the inviscid, sharp-cone pressure for p_i. A higher level of accuracy is especially desirable if C_L or C_M are being calculated.

The free-molecular pressure is calculated by means of Eq. (12),[9]

$$p_{fm}/p_\infty = [(1 + E)S_\infty(1/\sqrt{\pi})\cos\theta + 0.5(1 - E)\sqrt{T_w/T_\infty}] \times \exp(-S_\infty^2\cos^2\theta) + \{(1 + E)(0.5 + S_\infty^2\cos^2\theta) + 0.5(1 - E)\sqrt{T_w/T_\infty}\sqrt{\pi}S_\infty\cos\theta\}[1 + \mathrm{erf}(S_\infty\cos\theta)] \quad (12)$$

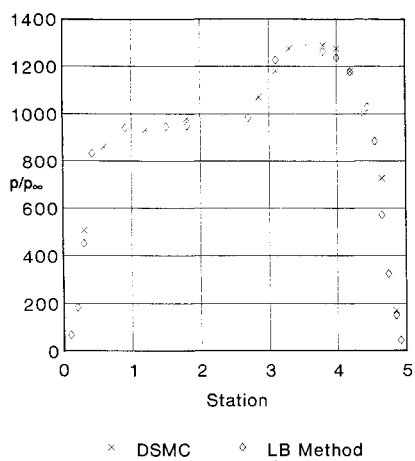

Fig. 8 Pressure ratio in vertical plane of symmetry of AFE vehicle at 110-km altitude predicted by present method and DSMC computations of Ref. 12.

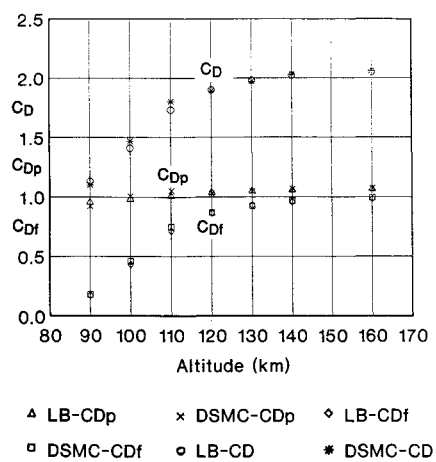

Fig. 9 Drag coefficients of 1.6-m-diam sphere at 7.5 km/s predicted by present method and DSMC computations of Ref. 4.

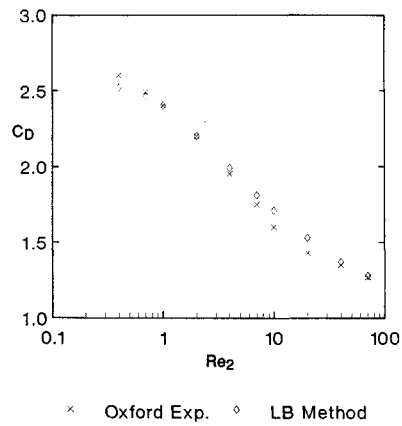

Fig. 10 Drag coefficients of spheres with $H_w = H_o$ and $M_\infty \approx 9$ predicted by present method and faired data from Ref. 13. Reynolds number based on sphere diameter.

Results and Discussion

The analysis and the bridging equations in the previous section are appropriate for hypersonic, transitional, rarefied flow over blunt-nosed convex, axisymmetric or quasi-axisymmetric (not two-dimensional) bodies. The stipulation excluding shapes that are of a two-dimensional character is necessary because the method has been developed on the basis of DSMC calculations for axisymmetric flows. The term quasi-axisymmetric is meant to encompass three-dimensional configurations comprised of transversely curved sections such that the local flow is like that over a tangent cone, e.g., the AFE or the blunt cone shapes at angles of attack.

Figures 3 and 4 show how C_p and C_f computed by the present local bridging method compare with results obtained by Moss[4] from DSMC solutions for flow over a sphere of 1.6-m diameter, with $T_w = 350$ K and a velocity of 7.5 km/s. Close agreement of the two methods at all sphere surface locations is apparent. That is also true of the results of both methods for all six other cases available in the DSMC sphere data.

Figure 5 gives a comparison of local friction coefficients computed for the 22.5-deg hyperboloid used as an example by Lee et al.[10] In this case, $M_\infty = 21.75$, $R_e = 16{,}930$/m, and nose radius $R_n = 0.0254$ m. The viscous shock layer (VSL) solutions assume a perfect gas, whereas the LB estimate is based on real-gas DSMC computations. It is not known if the offset in the C_f distribution near the nose in Fig. 5 is attributable to that difference. Otherwise, the agreement is satisfactory.

Figure 6 presents local shear stress computed for the vertical plane of symmetry of the "short" side of the AFE windward face (see Fig. 7) by the LB and DSMC[11] methods. In this example, $T_w = 1000$ K, Mach number is 36.0, and altitude is 90 km. Again, the general agreement of the DSMC and the LB methods is apparent.

Figure 8 shows a comparison of pressure distributions computed for the plane of symmetry of the face of the AFE vehicle. The DSMC results are from Ref. 12. Velocity is 9.9 km/s, wall temperature is 950 K, and the vehicle is at 17-deg angle of attack. The DSMC pressures have been read from a figure in the reference, so some small degree of inaccuracy is possible. Nonetheless, the level of agreement is satisfactory.

Figure 9 displays the results for drag coefficients of a 1.6-m-diam spherical body at 7.5 km/s and $T_w = 350$ K at various altitudes. The pressure, friction, and total drag coefficients are shown to illustrate their changes as altitude varies. The DSMC results are from Ref. 4.

All of the comparisons thus far have involved cold-wall conditions where the ratio H_w/H_o is very small. Figure 10 gives a comparison of results for the extreme case of $H_w = H_o$. The experimental data are sphere drag coefficients obtained from an unheated, hypersonic wind tunnel.[13] The post-

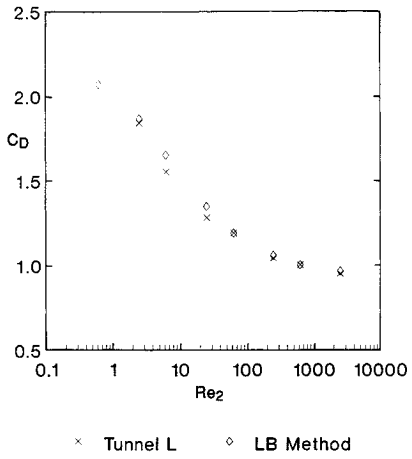

Fig. 11 Drag coefficients of spheres with $H_w = 0.086H_o$ and $M_\infty \approx 10.6$ predicted by present method and faired data from Ref. 14. Reynolds number based on sphere diameter.

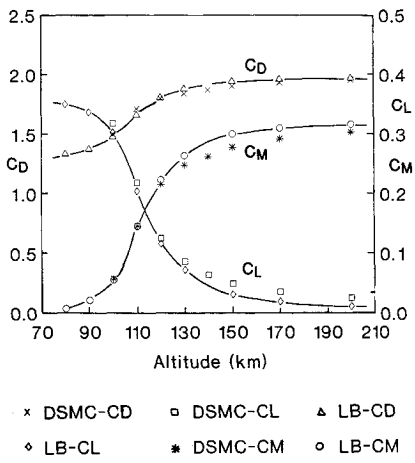

Fig. 12 Aerodynamic coefficients of AFE vehicle predicted by present method and DSMC computations of Ref. 12. Vehicle at 17-deg angle of attack, as shown in Fig. 7, and 9.9 km/s. Reference area $A = 14.2$ m^2, reference length $l = 4.26$ m.

shock Reynolds number Re_2 is defined as $(\rho U)_\infty d/\mu_2$ where d is sphere diameter. To the degree that this comparison of overall drag coefficients warrants, it appears that the influence of heat transfer on skin friction is adequately taken into account. Figure 11 shows another comparison of sphere drag results wherein the experimental data[14] correspond to $H_w/H_o = 0.086$ and $M_\infty = 10.6$. This furnishes a test case at an intermediate, cold-wall condition, and again the agreement is good. In both Figs. 10 and 11, the experimental data are represented by points from curves faired through the measured data. Therefore, experimental scatter is not evident.

Figure 12 compares drag, lift, and pitching moment coefficients computed by the LB method and the DSMC method[12] for the proposed AFE spacecraft shown in Fig. 7. Generally satisfactory agreement is shown. The moment reference point (MRP) of Fig. 7 was used in these calculations to enable comparison with the DSMC results. It should be mentioned that the LB and DSMC computer programs that link body geometry and aerodynamic calculations were different because the DSMC results are taken from Ref. 12 and the LB results were calculated by the present authors. One notable difference, for example, is the smaller number of surface area elements in the LB case, owing to use of a less powerful computer. It is possible that moment coefficient, in particular, could be affected by the number or distribution of elements in the surface grid.

Although the present LB method has been formulated for blunt-nosed and bluff bodies, it is of interest to learn if sharp-nosed or more slender shapes also can be considered. The application to bodies of greater fineness ratio may be tested by comparison to DSMC results for local skin friction and pressure on a blunt cone of 5-deg half-angle given in Ref. 15. These computed data were not used in formulating the LB method. The DSMC calculations include real air effects. Conditions are $U_\infty = 7.5$ km/s, $T_w = 1000$ K, and nose radius of curvature $R_n = 0.0254$ m.

The need to modify the local wall pressure to better approximate conical afterbody flow conditions has already been mentioned. Equation (11) is based on flow over a hemisphere. For this 5-deg cone, a method-of-characteristics solution has been used to obtain the inviscid, baseline pressure distribution on the cone frustum, but Eq. (11) was used for the nose.

Figure 13 shows the result of extending the LB method for C_f, and Fig. 14 presents the results for p/p_∞. Figure 15 compares overall C_D calculations for this body. Knudsen number is here defined as freestream mean free path divided by nose radius. The DSMC and VSL results are from Ref. 15. In regard to both local and overall results, the LB method leads to estimates in relatively good agreement with the more rigorous computational methods. At 50-km altitude, pressure drag dominates overall C_D, but at 100 km friction drag is the major component. The lower Kn case is in the category $Z < \Theta(1)$ for

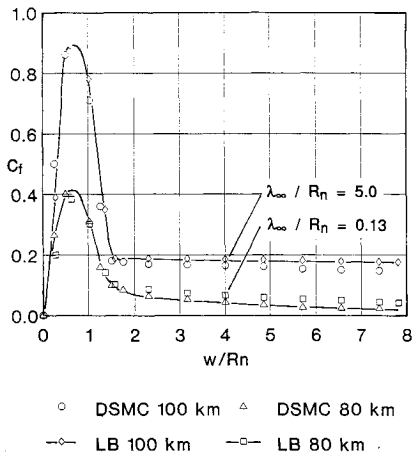

Fig. 13 Skin friction coefficients on blunt, 5-deg half-angle cone at 7.5 km/s and zero angle of attack. Nose radius = 0.0254 m. Comparison of present method and DSMC computations of Ref. 15.

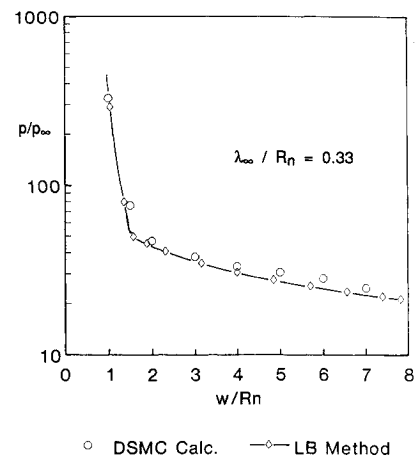

Fig. 14 Pressure distribution on blunt, 5-deg half-angle cone at 7.5 km/s, zero angle of attack, and 85 km altitude. Nose radius = 0.0254 m. Comparison of present method and computations of Ref. 15.

which there are no data in Fig. 1. Reasonable agreement with the DSMC calculations is shown at all higher Kn, where that method is the most accurate, and there is agreement with the VSL method at the lower Kn where that method should be reliable.

Despite the rather successful outcome in the case of the 5-deg blunt cone discussed earlier, it would not be justifiable to claim that the LB method will produce equally good estimates when applied to more slender or sharp-nosed shapes. The 5-deg cone has a nose-to-base radius ratio of 0.62, axial length-to-nose radius ratio of 7.87, wetted length-to-nose radius of ratio of 8.24, and a length-to-base diameter ratio of 2.45. Those proportions apparently qualify it as a blunt, bluff body not too far removed from the hemispheres and other bodies already discussed. This is supported by the pressure distribution in Fig. 14 that shows a negative gradient all along the cone. In this context, this body may serve to define an approximate upper limit of, say, $w/R_n \approx 10$ on "slenderness" permitted by the LB method as presented thus far. The evidence for that is the result of a comparison of total drag coefficients from experiments in two low-density, hypersonic wind tunnels and calculations by the LB method. These cones had wetted length-to-nose radius ratios of 15.7, 18.3, 24.0, and "infinity." The cone semi-apex angles varied from 6 to 15 deg. In every case, drag coefficient was underpredicted using the LB method. The lack of data on C_p or C_f in these experiments prevents a more detailed analysis of the discrepancies, but it is reasonable to assume that underprediction of C_f is the major factor.

The chief reason for expecting the need for a modification to the friction drag calculation is the $Re^{-1/2}$ "built in" when the parameter Z was based on a thin, laminar, boundary-layer analysis. This causes Z, and therefore C_f, to decrease as Re increases with length along a slender body. In the free-molecular limit and in transitional flow over bodies such as wedges or cones, C_f does not vary as $Re^{-1/2}$. The correlation shown in Fig. 1 is based on DSMC calculations for spheres, and it must be inferred that the combined body shape terms, $(1 + \sin\theta)/Re^{1/2}$, in Eq. (6) satisfactorily represent that type of bluff-body flow. However, the correlation apparently will need revision if it is extended to cases of $w/R_n > 10$. Otherwise, the result will be an underprediction of C_f on long afterbodies. Lacking an adequate amount of data for C_p and C_f on slender or sharp-nosed shapes, the correlation that led to the approximations given in the analysis section has not yet been broadened to accommodate slender shapes of greater w/R_n.

Returning to the case of the 5-deg blunt cone, the LB method also has been used to calculate lift and drag at angles of attack. Figure 16 presents lift-to-drag ratio for 20-deg angle of attack as a function of Knudsen number based on nose radius. The effect of increasing skin friction drag at high altitude is very clear. Unfortunately, there are no other data to compare with these results. In particular, the assumption in the calculations that local forces are negligible where $\theta > 90$ deg is worthy of more study when shapes such as this one are involved.

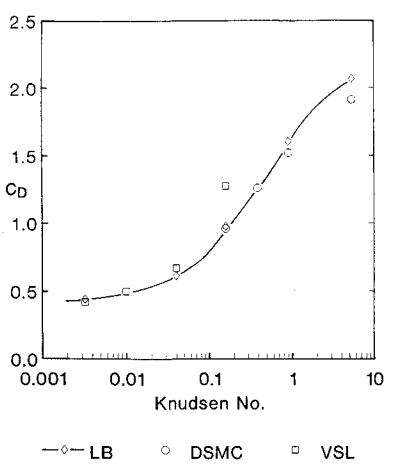

Fig. 15 Drag coefficients of blunt, 5-deg half-angle cone at 7.5 km/s and zero angle of attack. Knudsen number = λ_∞/R_n. DSMC and VSL results from Ref. 15.

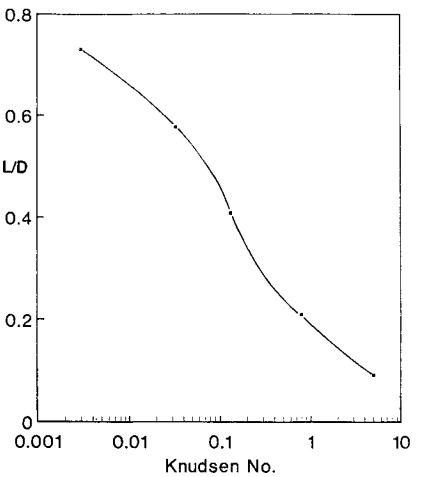

Fig. 16 Lift-to-drag ratio calculated by LB method for blunt, 5-deg cone at 20-deg angle of attack and 7.5 km/s. Knudsen number = λ_∞/R_n.

Conclusions

The LB procedure described herein is based on a correlation of local friction and pressure coefficients computed for real-gas flow over spheres by the DSMC technique. Various examples of results of computations by the LB and DSMC methods have been presented to enable an evaluation of the accuracy of the LB method relative to the DSMC method when applied to "bluff" shapes here defined by $w/R_n < 10$. Although the limitation to bluff shapes is repeatedly emphasized in this paper, comparisons of the LB and DSMC results indicate that, within this restriction, the LB method offers a comparatively simple and rapid means for predicting approximate aerodynamic coefficients when the DSMC approach is not available or not feasible, e.g., in optimization studies. The ability to predict local coefficients on bodies allows aerodynamic load distribution and moment coefficients to be estimated.

Acknowledgments

This work has been supported by NASA Research Grants NAG 1-878 and NAG 1-921, with B. T. Upchurch and R. C. Blanchard the respective NASA technical officers. Of the several NASA engineers whose generous contributions of data made this work possible, J. N. Moss, J. F. Alison III, R. C. Blanchard, and C. M. Seaford deserve particular recognition. The assistance of Paul A. Skoglund and J. Kent Rockaway, undergraduate research assistants at Vanderbilt University, has been very valuable.

References

[1]Potter, J. L., Kinslow, M., Arney, G. D., and Bailey, A. B., "Initial Results from a Low-Density, Hypervelocity Wind Tunnel," *Hypersonic Flow Research,* edited by F. R. Riddell, Academic Press, New York, 1962, pp. 599–624.

[2]Kotov, V. M., Lychkin, E. N., Reshetin, A. J., and Schelkonogov, A. N., "An Approximate Method of Aerodynamics Calculation of Complex Shape Bodies in a Transition Region," *Rarefied Gas Dynamics,* edited by O. M. Belotserkovskii, M. N. Kogan, S. S. Kutateladze, and A. K. Rebrov, Vol. 1, Plenum Press, New York, 1985, pp. 487–494.

[3]Xie, Y., and Tang, Z., "Approximate Calculation of Rarefied Aerodynamic Characteristics of Convex Axisymmetric Configura-

tions," *Rarefied Gas Dynamics,* edited by E. P. Muntz, D. P. Weaver, and D. H. Campbell, Vol. 118, Progress in Astronautics and Aeronautics, AIAA, Washington, DC, 1989, pp. 476–483.

[4]Moss, J. N., personal communication, NASA Langley Research Center, Hampton, VA, 1990.

[5]Cohen, C. B., and Reshotko, E., "The Compressible Laminar Boundary Layer with Heat Transfer and Arbitrary Pressure Gradient," NACA Rept. 1294, 1956.

[6]Hurlbut, F. C., "Particle Surface Interaction in the Orbital Context: A Survey," *Rarefied Gas Dynamics, Space-Related Studies,* edited by E. P. Muntz, D. P. Weaver, and D. H. Campbell, Vol. 116, Progress in Astronautics and Aeronautics, AIAA, Washington, DC, 1989, pp. 419–450.

[7]Kogan, M N., *Rarefied Gas Dynamics,* translation editor L. Trilling, Plenum Press, New York, 1969, pp. 454–473.

[8]Touloukian, Y. S. (ed.), *Thermophysical Properties of Matter,* TPRC Data Series, Plenum Press, New York, 1975, pp. 512–611.

[9]Bird, G. A. *Molecular Gas Dynamics,* Clarendon Press, Oxford, England, UK, 1976, p. 93.

[10]Lee, K. P., Gupta, R. N., Zoby, E. V., and Moss, J. N., "Hypersonic Viscous Shock-Layer Solutions over Long Slender Bodies—Part II: Low Reynolds Number Flows," *Journal of Spacecraft and Rockets,* Vol. 27, No. 2, 1990, pp. 185–191.

[11]Moss, J. N., and Price, J. M., "Direct Simulation of AFE Forebody and Wake Flow with Thermal Radiation," NASA TM 100673, Sept. 1988.

[12]Celenligil, M. C., Moss, J. N., and Blanchard, R. C., "Three-Dimensional Flow Simulation About the AFE Vehicle in the Transitional Regime," AIAA Paper 89-0245, Jan. 1989.

[13]Hadjimichalis, K. S., and Brundin, C. L. "The Effect of Wall Temperature on Sphere Drag in Hypersonic Transition Flow," *Rarefied Gas Dynamics,* Vol. 2, edited by M. Becker and M. Fiebig, DFVLR Press, Porz-Wahn, Germany, 1974.

[14]Kinslow, M., and Potter, J. L., "Drag of Spheres in Rarefied Hypervelocity Flow," *AIAA Journal,* Vol. 1, No. 11, 1963, pp. 2467–2473.

[15]Moss, J. N., Cuda, V., Jr., and Simmonds, A. L., "Nonequilibrium Effects for Hypersonic Transitional Flows," AIAA Paper 87-0404, Jan. 1987.

Gerald T. Chrusciel
Associate Editor